Available online at www.eccomasproceedia.org
Eccomas Proceedia COMPDYN (2017) 3281-3296

ECCOMAS
Proceedia

-COMPDYN 2017
6th ECCOMAS Thematic Conference on
Computational Methods in Structural Dynamics and Earthquake Engineering
M. Papadrakakis, M. Fragiadakis (eds.)
Rhodes Island, Greece, 15–17 June 2017

DEFINITION OF A FIBER MACRO-MODEL FOR NONLINEAR ANALYSIS OF INFILLED FRAMES

F. Di Trapani[1]*, L. Cavaleri[2], G. Bertagnoli[1], G. Mancini[1], D. Gino[1], M. Malavisi[1]

[1]Politecnico di Torino
Department of Structural, Geotechnical and Building Engineering
Corso Duca degli Abruzzi 24 - Torino
fabio.ditrapani@polito.it, gabriele.bertagnoli@polito.it, giuseppe.mancini@polito.it, diego.gino@polito.it, marzia.malavisi@polito.it

[2] University of Palermo
Dipartimento di Ingegneria Civile, Ambientale, Aerospaziale, dei Materiali
Viale delle Scienze 90128 - Palermo
liborio.cavaleri@unipa.it

Keywords: Infilled frames, fiber-section elements, micromodelling, macromodelling, FEM, stress-strain, correlations.

Abstract. *A common way to model infill-frame interaction is the use equivalent strut macro-models. In most cases these are compression only resistant truss elements defined with a multi-linear axial-force / axial-displacement law. The main difficulty in using this approach is to correctly calibrate such a force-displacement curve (slope of ascending and post-peak branches, critical yielding, peak and residual forces) because of the large number of variables (mechanical and elastic properties of materials) and the different possible damage mechanisms activated for the frame-infill system. Another possible way is using fiber-section elements as diagonal struts. In this case the force-displacement law is substituted by a stress-strain curve. In both cases a reliable definition of inelastic response of the strut, based on mechanical approaches, which are valid in general is not easy, as most of models provide rules valid for specific typologies of infills (e.g. weak or strong infills) and frames (e.g. concrete or steel frames). Based on this, the paper proposes the use of fiber-section diagonal struts with a concrete-type stress-strain relationship calibrated using a semi-empirical approach. The Kent-Scott-Park model, depending on four parameters, is used as reference constitutive law for the strut. Experimental data and additional numerical simulations are used to derive semi-empirical correlations linking geometrical and mechanical properties of the frame-infill system to the aforementioned parameters governing nonlinear response of the diagonal. Analytical expressions of the best fitting curves are finally provided and suggested as design equation.*

Peer-review under responsibility of the organizing committee of COMPDYN 2017.
doi: 10.7712/120117.5645.18525

1 INTRODUCTION

Infilled frames are typically placed in framed structures as partition walls and to separate internal spaces from external environment. Although they are not commonly included in structural models, laboratory tests [e.g.1-4] and real observation of post-earthquake damage have demonstrated that masonry infills have a strong interaction with primary structures, influencing overall and local strength, stiffness and structural ductility [5-7]. Basically two different approaches are used to model infill-frame interaction. One is detailed finite element 2D or 3D modeling (e.g [8-10]) of the infill, the frame and the interface mortar [11-14]. Such a kind of approach is generally preferred for research purposes as it requires significant computational effort and expertise of the user. The other is macromodelling of the infill, which provides the use of one (or more) equivalent diagonal struts. This is approach is largely employed, especially when performing seismic assessments using nonlinear static or dynamic analyses. Since equivalent struts are an idealization of the real system, they have to undergo an identification process in order to effectively simulate the infill-frame interaction. A number of identification methods have been developed in the last 60 years. Some of these focused on the stiffening effects [15-19] produced by the infills on the overall response, other studies [e.g. 20-22] were addressed to the assessment of the inelastic in-plane response. More recently, equivalent strut macromodels have been updated to include the possibility to model the out-of-plane response of the infill wall, and its mutual interaction with the in-plane damaging. Studies [e.g. 23-25] have demonstrated that infills can develop a significant resistance against out-of-plane actions if they have adequate thickness and the frame is stiff enough. An updated literature review of macromodelling techniques can be found in [26].

Although, as it can be seen, a large literature is available, the uncertainty in the identification of the equivalents struts, in particular their inelastic response, still remains an open issue. This is due to the fact that the overall lateral response of the infilled frame basically depends on the damage mechanism occurring from time to time, which in turns, as summarized in [1], depends on the different possible assemblage of masonry infills and frames. Because of this, sliding of mortar joints, rather than corner crushing of units, of diagonal failure may occur. Moreover, in many cases, a combination of such mechanisms is also observed.

Such potential variability of failure mechanisms is not easy to predict a priori, and still constitutes the main unknown in the assessment of such systems. In fact, the identification strategies available in literature, which make use of mechanical approaches to predict the inelastic response are generally referred to special typologies of infilled frames or validated with reduced experimental testing. Consequently, a strategy to define the inelastic behaviour of the equivalent strut, which can be considered to be valid for any typology of masonry and any typology of frame, is not yet available in the literature. Today, the increasing need for a reliable assessment of seismic performance of new and existing buildings [27-32] moves the interest in finding models which are accurate in reproducing the inelastic response of structures.

Based on the aforementioned difficulties encountered in using mechanical approaches to define nonlinear behaviour of the equivalent struts, this paper proposes a calibration strategy making use of a semi-empirical definition of the parameters governing their inelastic response. The procedure is based on the use fiber-section elements to model equivalent struts, associating a concrete-type (Kent-Park [33]) stress-strain model for the fibers. This stress-strain model is basically governed by four parameters: peak strength, peak strain, ultimate strength and ultimate strain.

A comparison between real experimental test results of different typologies of specimens of infilled frames, and results of the associated equivalent strut models, allowed iteratively calibrating the four stress-strain parameters for several specimens. The same calibration pro-

cedure was repeated with the results of a detailed FE model. After, analytical correlation laws, based on the interpolation of data obtained, linking geometrical and mechanical features of an infilled frame and the stress-strain parameters were provided. The latter can be used as predictive tool for the identification of the stress strain law to assign to the equivalents struts.

2 PROPOSED MODELLING STRATEGY AND DETERMINATION OF THE STRESS-STRAIN PARAMETERS

The identification method proposed, is aimed at the definition of the stress-strain law to be assigned to the equivalent struts of a generic infilled frame. This implies that struts are modeled using fiber-section elements. The reference numerical models used in the paper are realized with OpenSees software platform [34]. The typical infilled frame model (Figure 1a-b) consists of nonlinear beam-column elements as beams and columns, and nonlinear compression only trusses as equivalent diagonal struts. The modeling scheme is shown in Figure 1b. The stress-strain law of the fibers composing the struts is a simple Kent-Park [33] concrete-type model. The latter depends on 4 parameters: peak strength (f_{md0}), peak strain (ε_{md0}), ultimate strength (f_{mdu}) and ultimate strain (ε_{mdu}) which regulate the ascending and descending branches. After the achievement of the ultimate strain the ultimate stress is maintained constant.

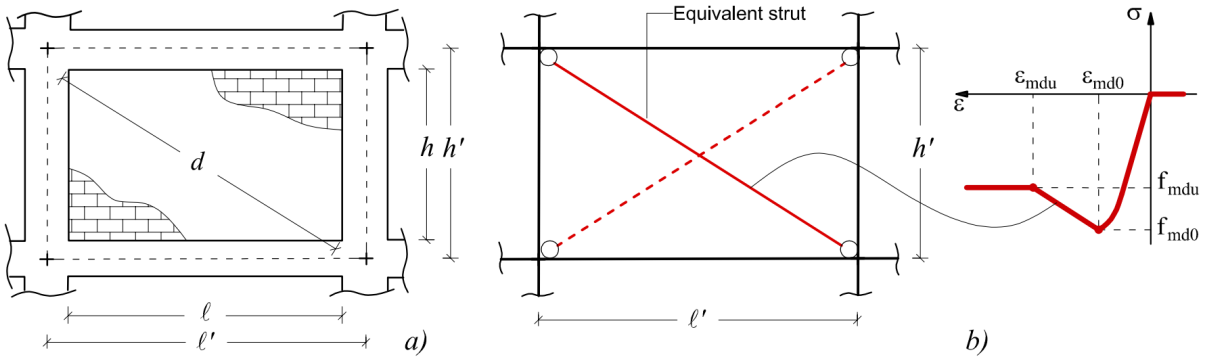

Figure 1: Modeling of an infilled frame: a) Real configuration; b) Equivalent strut model.

When using this approach to model equivalent struts, it should be noted that the four stress-strain parameters (f_{md0}, ε_{md0}, f_{mdu}, ε_{mdu}) are not coincident with those associated with the masonry constituting the infill. This is due to the fact that the lateral response of an infilled frame depends on the damage mechanism typology rather directly on masonry properties. As example, if the failure mechanism activated is the sliding of mortar joints, it is reasonable that compressive strength of masonry will be not achieved. For this reason, the stress-strain parameters, and the associated stress-strain relationship have to be intended as purely phenomenological. However, the stress-strain parameters cannot be thought as non-correlated with masonry properties, but more in general they depend on the geometrical and mechanical properties of the overall system.

The aim of the paper is then to find four analytical correlations which allow, starting from the basic geometrical and mechanical data of an infilled frame, to determine each of the stress-strain parameters. In this way once the infilled frame features are defined, the stress-strain curve of the struts can be evaluated through simple analytical calculations.

In order to derive the aforementioned correlations, the following procedure has been implemented:

1. Acquisition of experimental test data (force-displacement curves of in-plane monotonic or cyclic tests on infilled frames);
2. Definition of the numerical models of the infilled frames actually tested;
3. Calibration of the parameters f_{md0}, ε_{md0}, f_{mdu}, ε_{mdu} iterating results of pushover curves up to the best matching with experimental curves;
4. Research of a correlation of between the stress-strain parameters obtained and the characteristics of the infilled frames.

Experimental calibration is considered the best way to derive stress-strain parameters, as it includes real phenomena which are not easily captured by analytical models. However, despite several researchers have conducted experiments on the in-plane response of infilled frames, only a few of these report detailed information on the preliminary tests on masonry (e.g. results of compressive tests on prisms, results of diagonal compressive tests, experimental evaluation of elastic and tangential moduli).

Because of this, in order to enlarge the data-set used to derive correlations, detailed FE models of the infilled frames actually testes were also realized. The FE models, once calibrated, were used to derive numerical predictions of the responses of the infilled frames with varying geometric and mechanical parameters of the infill. The subsequent procedure has been followed:

1. Calibration of a detailed FE model with experimental data;
2. Variation of geometrical and mechanical properties and derivation of numerical lateral force-displacement curves;
3. Definition of the OpenSees models of the infilled frames tested in FE simultions;
4. Calibration of the parameters f_{md0}, ε_{md0}, f_{mdu}, ε_{mdu} iterating results of pushover curves up to the best matching with numerically generated curves;
5. Adding data to those obtained with experimental calibration.

Stress-strain parameters data-sets, one obtained from experimental tests, the other from numerical simulations of detailed FE models were then merged.

In the aforementioned process, the identification of the cross-section dimensions of the equivalent strut is carried is carried out using the procedure by Asteris et al. [19], which briefly summarized in the following. According to [19], the thickness (t) is equal to the actual thickness of the infill, while the width (w) is evaluated as:

$$w = k^{\gamma}\left(\frac{h}{l}\right)\frac{c}{\lambda^{*\beta}}d \tag{1}$$

where, with reference to Figure 1, d is the length of the diagonal strut, h and l are the length and the height of the infill, κ is a parameter accounting for the stiffening action exerted by vertical loads, defined as:

$$\kappa = [1 + (\lambda^{*} + 200)\varepsilon_{v}] \tag{2}$$

in which ε_v is the axial strain on columns, calculated considering the total load F_v acting on the 2 columns having cross-sectional area A_c and elastic modulus E_c, as:

$$\varepsilon_{v} = \frac{F_{v}}{2E_{c}A_{c}} \tag{3}$$

The parameter λ^{*} is calculated with the expression by Papia et al. (2003) [35]:

$$\lambda^* = \frac{E_{md}}{E_c}\frac{th'}{A_c}\left(\frac{h'^2}{l'^2}+\frac{1}{4}\frac{A_c}{A_b}\frac{l'}{h'}\right) \tag{4}$$

where E_{md} is the Young modulus of the masonry infill along the diagonal direction and A_b is the area of the beam cross-section. The other symbols appearing in Eq. (4) can be simply deduced from Figure 1.

The parameter γ in Eq. (1) takes into account the combined effect of openings and aspect ratio with the following expression:

$$\gamma = 1 + 0{,}5\frac{r}{(l/h)^4} \tag{5}$$

being $r=1$ for in the case of solid infills.

Finally c and β depend on the Poisson's ratio ν_d of the masonry constituting the infill along the diagonal direction according to the following expressions:

$$\begin{aligned} c &= 0{,}249 - 0{,}0116\nu_d + 0{,}567\nu_d^{\,2} \\ \beta &= 0{,}146 - 0{,}0073\nu_d + 0{,}126\nu_d^{\,2} \end{aligned} \tag{6}$$

The determination of E_d and ν_d starting from elastic moduli along the 2 orthogonal directions is described in [2]. In absence of experimental data in both directions the average Young's modulus and Poisson's ration along the vertical direction are used.

3 STRESS-STRAIN PARAMTERS FROM EXPERIMENTAL TESTS

Experimental test data from Cavaleri and Di Trapani (2014) [22], Mehrabi et al. (1996) [1], Kakaletsis and Karayannis [3], Papia et al. [35] were used as reference to derive stress-strain parameters. The choice of these studies was due to the completeness of their experimental programs, which included also detailed data of experimental tests on masonry constituting infills. Design details of specimens are reported in Table. 1.

The widths of the equivalent strut models associated to the specimens are also reported in Table 2 together with the parameters for their identification, calculated according to [19] and [35].

Auth.	Spec. #	Masonry. Typol.	t (mm)	h (mm)	h' (mm)	l (mm)	l' (mm)	l/h	d (mm)	A_c (mm²)	A_b (mm²)
[22]	S1A	Calc.	200	1600	1800	1600	1800	1.0	2545.6	40000.0	80000.0
[22]	S1B	Clay.	150	1600	1800	1600	1800	1.0	2545.6	40000.0	80000.0
[22]	S1C	LW conc.	300	1600	1800	1600	1800	1.0	2545.6	90000.0	120000.0
[1]	4	Brick	92	1422	1536	2032	2210	1.43	2691.5	31684.0	34838.6
[1]	5	Brick	92	1422	1536	2032	2210	1.43	2691.5	31684.0	34838.6
[1]	11	Brick	92	1422	1536	2948	3126	2.07	3483.1	31684.0	34838.6
[1]	6	Brick	92	1422	1536	2032	2235	1.43	2712.3	41290.2	34838.6
[3]	S	Brick	60	800	900	1200	1350	1.5	1622.5	22500.0	20000.0
[35]	S2A	Calc.	200	1600	1800	1600	1800	1.0	2545.6	40000.0	80000.0
[35]	S2B	Lat.	150	1600	1800	1600	1800	1.0	2545.6	40000.0	80000.0

Table 1: Geometric details of specimens tested by [1], [3], [22], [35].

Auth.	F_v (kN)	E_{md} (N/mm²)	E_c (N/mm²)	v_d -	c -	β -	ε_v -	κ -	r -	γ -	h/l -	λ^* -	w (mm)
[22]	400	5670	25000	0.15	0.260	0.150	0.00020	1.048	1	1.50	1.00	2.30	627.1
[22]	400	5719	25000	0.10	0.254	0.148	0.00020	1.046	1	1.50	1.00	1.74	636.4
[22]	400	3254	25000	0.18	0.264	0.151	0.00009	1.019	1	1.50	1.00	0.93	700.4
[1]	294	4600	17000	0.15	0.260	0.150	0.00027	1.059	1	3.08	0.70	0.98	587.1
[1]	294	8949	18064	0.15	0.260	0.150	0.00026	1.060	1	3.08	0.70	1.79	536.6
[1]	294	9604	18133	0.15	0.260	0.150	0.00026	1.059	1	10.24	0.48	1.66	726.7
[1]	294	4198	19856	0.15	0.260	0.150	0.00018	1.038	1	3.08	0.70	0.65	590.1
[3]	100	660	29961	0.15	0.260	0.150	0.00007	1.015	1	3.53	0.67	0.05	470.5
[35]	400	8317	23000	0.09	0.253	0.148	0.00022	1.058	1	1.50	1.00	3.66	577.4
[35]	400	5719	23000	0.10	0.254	0.148	0.00022	1.051	1	1.50	1.00	1.89	632.8

Table 2: Mechanical data of specimens and identification parameters.

The experimental tests were simulated with the OpenSees models, iterating the stress-strain parameters associated with the equivalent struts in order to best-fit the experimental backbone curves. The results obtained after the calibration of the equivalent struts are shown in Figures 2-5.

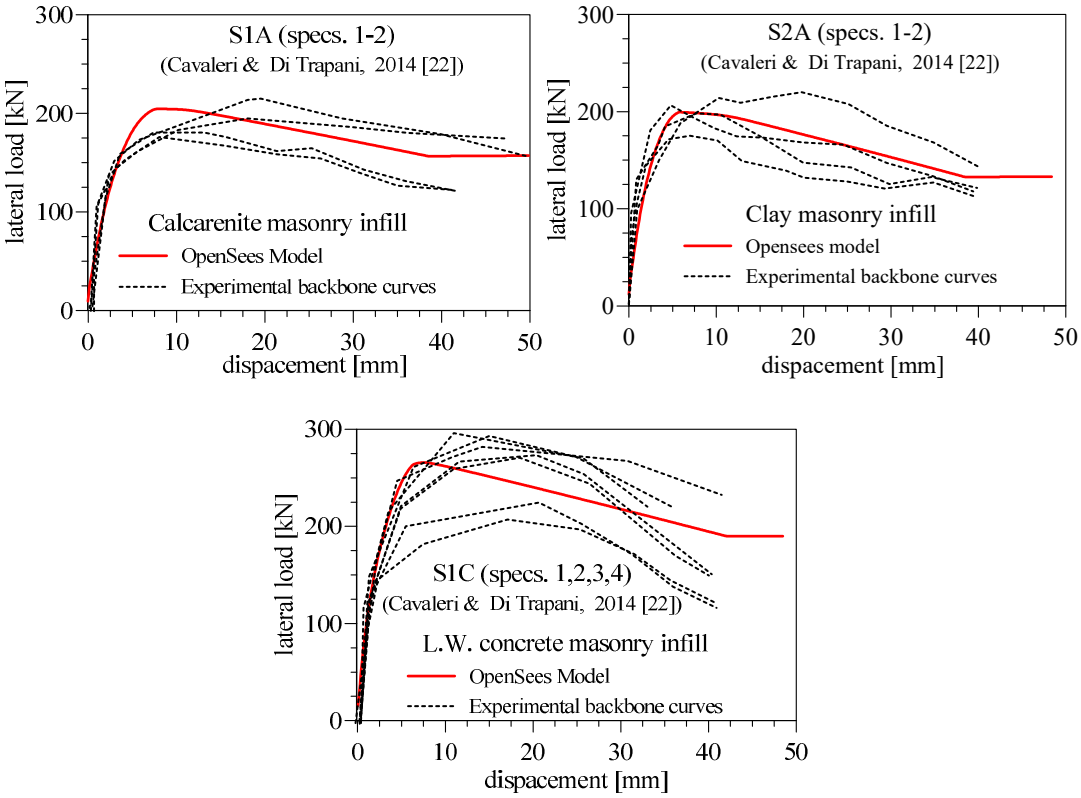

Figure 2: Experimental backbone curves of specimens by Cavaleri and Di Trapani, 2014 [22] and pushover curves of the OpenSees model at the end of the calibration.

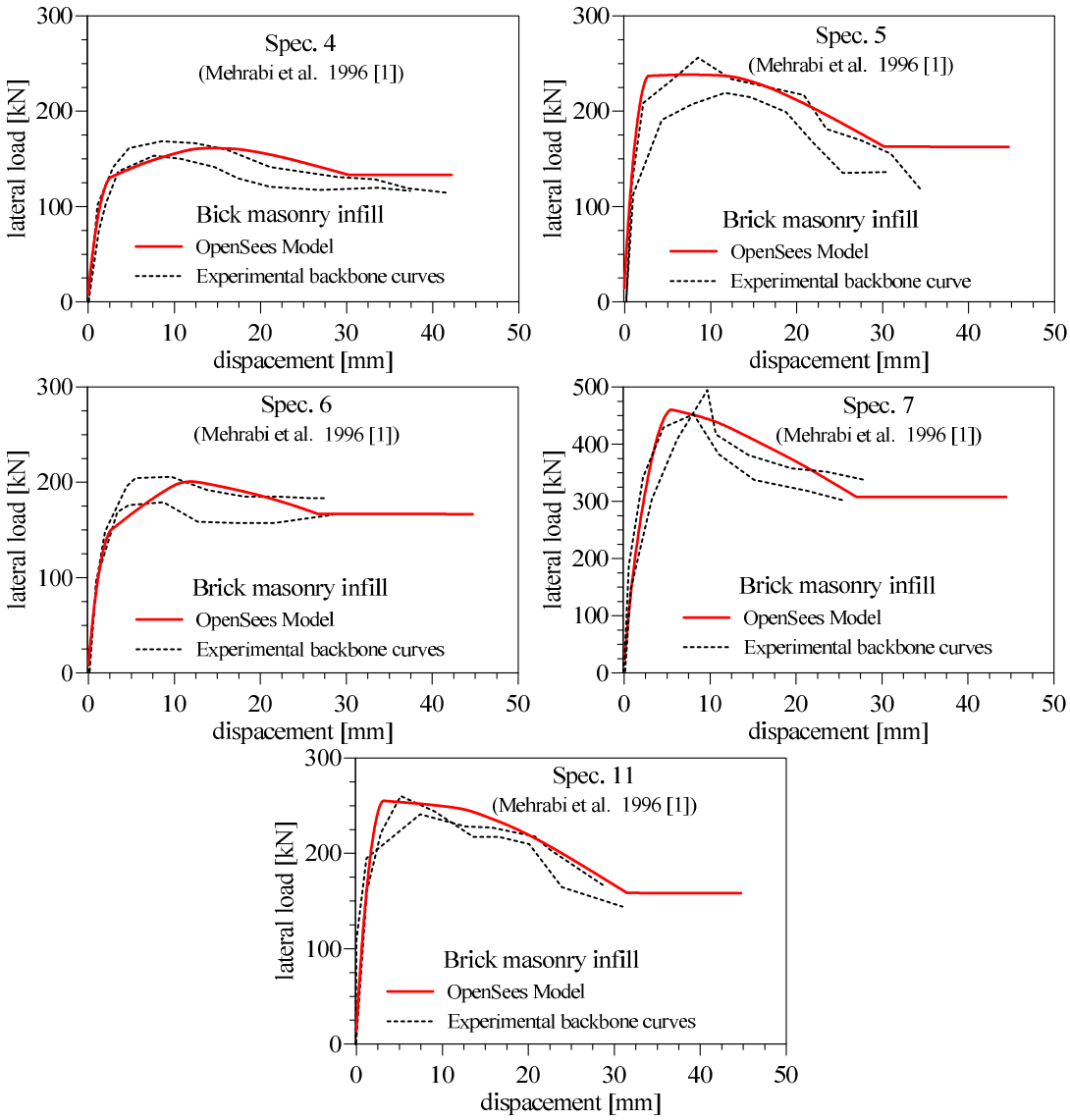

Figure 3: Experimental backbone curves of specimens by Mehrabi et al., 1996 [1] and pushover curves of the OpenSees model at the end of the calibration.

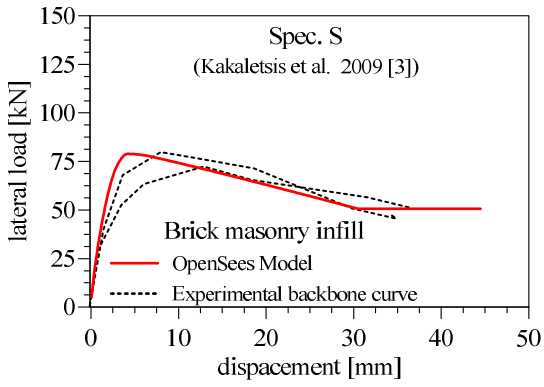

Figure 4: Experimental backbone curves of specimens by Kakaletsis et al., 2009 [3] and pushover curves of the OpenSees model at the end of the calibration.

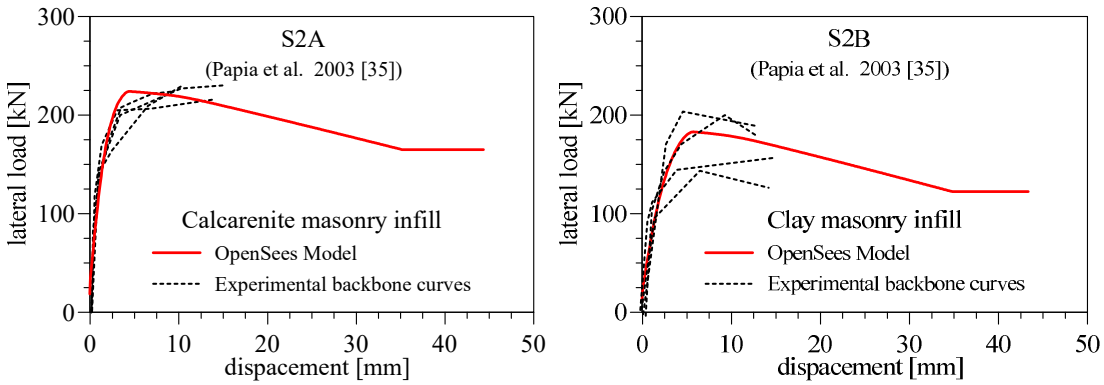

Figure 5: Experimental backbone curves of specimens by Papia et al., 2003 [35] and pushover curves of the OpenSees model at the end of the calibration.

The stress-strain parameters obtained for the models of the infilled frame specimens analyzed are reported in Table 3, together with the experimental values of shear and compressive strength of masonry infills. It can be observed, as before mentioned, that the compressive strength of diagonal struts (f_{md0}), which resulted after the calibration, was significantly lower than the actual compressive strength (f_{mdu}). This reduction ranged between -25% and -75% and depended on the different damage mechanism actually activated during the tests.

The experimental/numerical comparisons have also shown that the use of diagonal fiber-section struts with a concrete-type stress-strain law is particularly suitable to predict the response of infilled frames. In particular the proposed modeling approach resulted particularly accurate in predicting the ascending and descending branches, regulating initial and post-cracking stiffness and post-peak softening.

Auth.	**Spec. #**	f_{vm}	f_m	f_{md0}	f_{mdu}	ε_{md0}	ε_{mdu}
		N/mm²	N/mm²	N/mm²	N/mm²	-	-
[22]	S1A	0.73	2.67	2.00	1.20	0.0018	0.0100
[22]	S1B	1.07	8.66	2.50	1.10	0.0015	0.0090
[22]	S1C	0.30	1.74	1.20	0.50	0.0015	0.0100
[1]	4	0.93	5.30	2.40	0.65	0.0008	0.0090
[1]	5	1.15	13.85	5.30	1.60	0.0008	0.0090
[1]	11	1.03	11.44	3.80	0.95	0.0008	0.0080
[1]	6	0.70	5.06	2.60	0.65	0.0008	0.0090
[3]	S	0.08	2.63	2.30	0.75	0.0030	0.0110
[35]	S2A	0.89	4.57	2.50	1.40	0.0010	0.0100
[35]	S2B	1.07	8.66	2.30	1.10	0.0015	0.0090

Table 3: Mechanical data of masonry and stress-strain parameters.

4 STRESS-STRAIN PARAMTERS FROM FE MODELS

In order to enlarge the data-set necessary to derive the correlations, additional tests were simulated with a detailed finite element model. The FE model was realized using ATENA 2D software platform which is based on a concrete smeared cracking model and also implements frictional interface elements. The reference specimens used for the simulation of the tests were specimens S1B [22]. Reinforced concrete elements were modeled using CCIsoQuad nonlinear elements with a SBeta material, defined with a uniaxial stress-strain concrete law and a biaxial failure criterion. The same material was used to model masonry units. Interface elements were used to model the contact surfaces between concrete and masonry and between masonry units. Interfaces were governed by Mohr-Coulomb failure surface with a specified friction coefficient and cohesion. Longitudinal reinforcement was included in the model using

rebar elements consisting in 1D truss with uniaxial steel (elasto-plastic with strain hardening law). For the transversal reinforcement a smeared reinforcement material was adopted. The numerical simulation of the tests consisted of two steps. First vertical loads at the tops of the column were applied. Then a lateral displacement was imposed up to the prescribed magnitude. The FE model and the assembly scheme are shown in Figure 6.

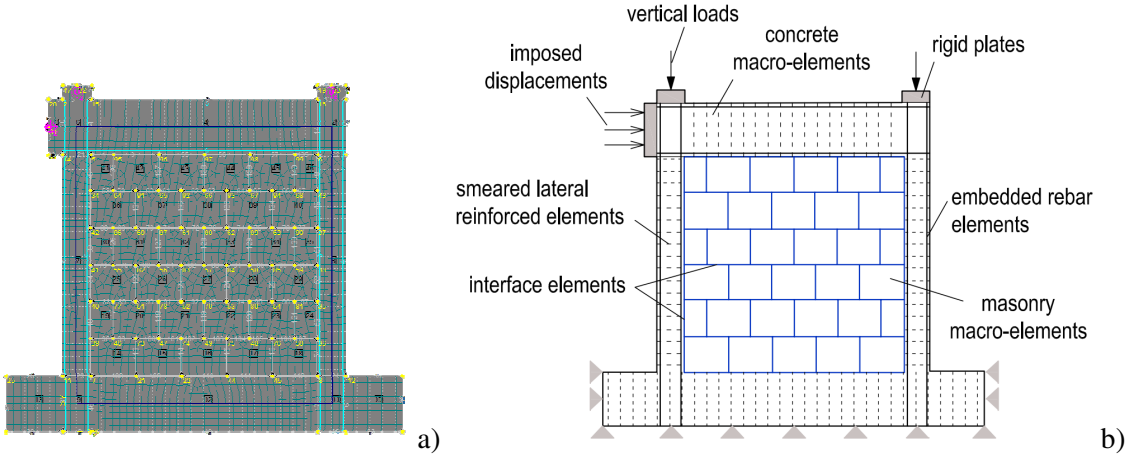

Figure 6: Definition of the FE model: a) FE model in ATENA; b)Scheme of the model assembly and application of loads.

The simulation of the tests of S1B specimen was iterated several times to obtain calibration parameters of the FE model. In the calibration process, mechanical data of materials (compressive and tensile strength of concrete and masonry) were those experimentally evaluated. The final result, after the calibration, is illustrated in Figure 7, where it can be noted the accuracy of the FE model in predicting the average initial stiffness and post-peak decay actually exhibited by the specimens. In Figure 8-a is shown the distribution of Von Mises stresses at the peak-load, while Figure 8-b and 8-c show the cracking pattern of the FE model at the peak and at the end of the test respectively. As it can be observed sliding of mortar joint was the dominant damage mechanism (as recognized in actual test), however this was associated with a diagonal cracking pattern involving masonry units. The calibration parameters determined for the reference FE model are reported in Table 4.

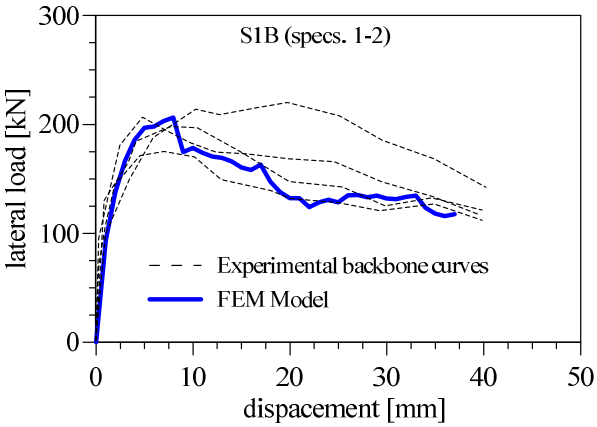

Figure 7: Experimental backbone curves of specimens S1B [35] and pushover curve of the FE model at the end of the calibration.

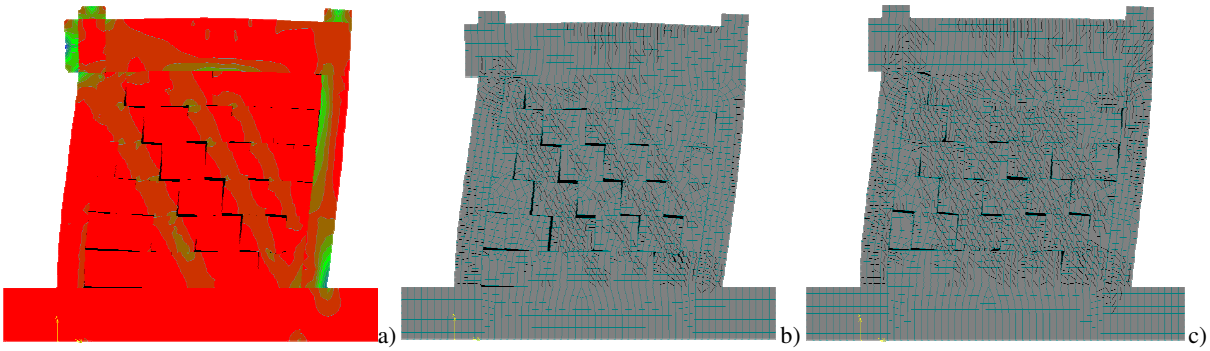

Figure 8: Results from FE model: a) Von Mises stresses at peak-load; b) cracking pattern at the peak-load; c) cracking pattern at end of the test.

Concrete				
Compressive strength	Tensile strength	Softening coefficient	Ultimate tensile strain	Shear retention factor
f_c [MPa]	**f_t [MPa]**	**-**	**-**	**-**
25	0.25	0.20	0.001	0.20
Masonry				
Compressive strength	Tensile strength	Softening coefficient	Ultimate tensile strain	Shear retention factor
f_{cm} [MPa]	**f_{vm} [MPa]**	**-**	**-**	**-**
8.66	1.07	0.20	0.001	0.15
Interface				
Normal stiffness	Tangential stiffness	Tensile strength	Cohesion	Friction coefficient
K_{nn} [MN/m]	**K_{tt} [MN/m]**	**f_t [MPa]**	**c**	**μ**
4000000	400000	0.4	1.0	0.7

Table 4: Mechanical data and calibration parameters of the reference FE model.

The FE model, after the calibration, was used to simulate supplementary tests by varying geometric and mechanical parameters of the infill. In particular the calibration parameters were fixed, as well as the geometry of the frame, while it was supposed to vary compressive and shear strength of masonry, infill thickness and masonry elastic modulus. The supplementary tests simulated are listed in Table 5, where the parameters each time varied are highlighted.

Spec. #	**f_{vm}** N/mm²	**f_m** N/mm²	**t** N/mm²	**E_m** N/mm²
FEM-1S	**0.60**	**12.00**	150	5719
FEM-2S	**0.40**	**4.00**	150	5719
FEM-3S	**0.20**	**2.00**	150	5719
FEM-1T	0.50	8.66	**50**	5719
FEM-1T	0.50	8.66	**100**	5719
FEM-1T	0.50	8.66	**150**	5719
FEM-1T	0.50	8.66	**200**	5719
FEM-1E	0.50	8.66	150	**1200**
FEM-2E	0.50	8.66	150	**2000**
FEM-3E	0.50	8.66	150	**3850**
FEM-4E	0.50	8.66	150	**9000**

Table 5: Geometric and mechanical data of numerical models generated from the reference S1B model.

The results of the tests simulated with the FE models are shown in Figure 9. Some general trends can be observed from the curves obtained, in particular: an increase of compressive and shear strength of masonry resulted in an global increase of the strength of the system, with a post-peak branch characterized by losses and regain of strength; an increase of the thickness of the infill resulted in an overall increase of strength, but this was less relevant as the thick-

ness increased, at the same time a post-peak loss of strength, progressively increasing, was recognized; an increase of Young's modulus of the infill resulted in a proportional increase of stiffness of the system and a significant reduction of the peak-displacement with a simultaneous reduction of the overall strength.

In Figure 9, results of the OpenSees models simulating FE tests are also reported. The parameters evaluated for the identification of the equivalent strut widths are reported in Table 6 together with the stress-strain parameters obtained after the calibration.

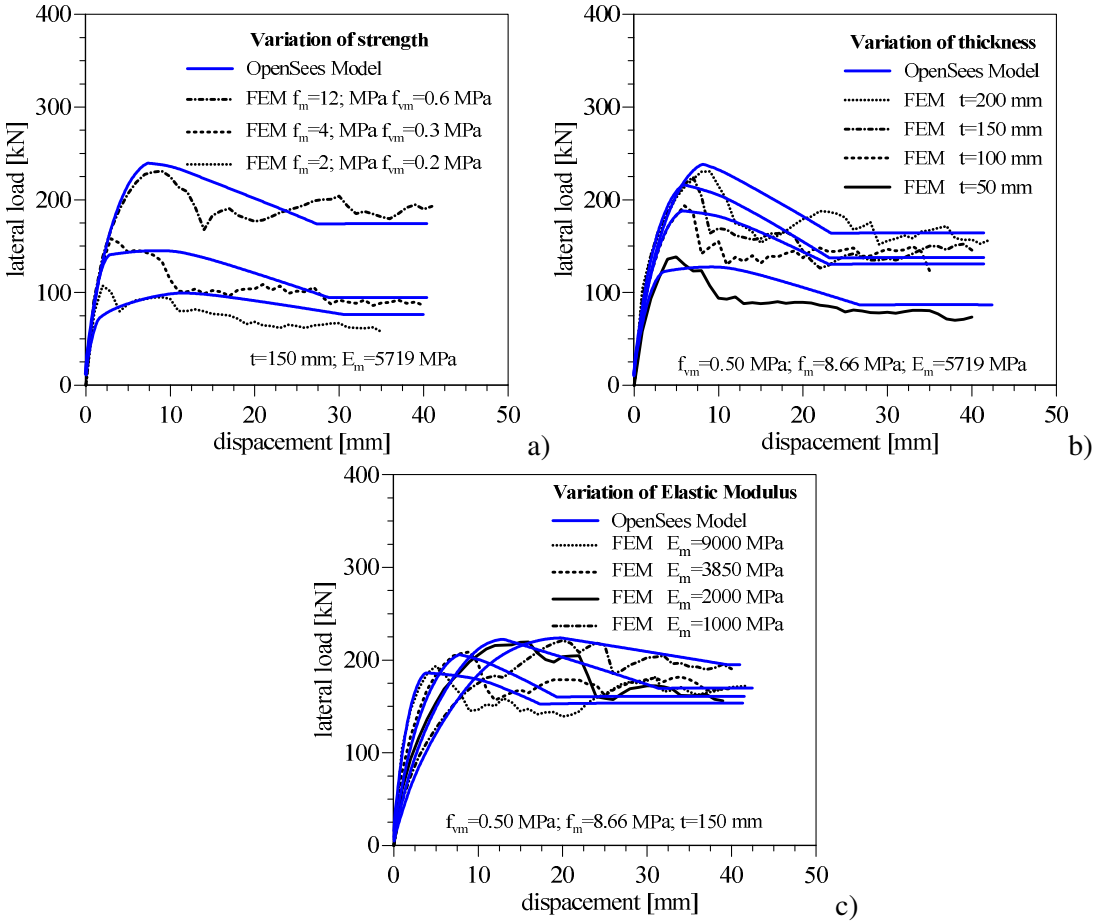

Figure 9: Results of FE model simulations and pushover curves of the OpenSees models at the end of the calibration: a) variation of strength; b) variation of thickness of the infill; c) variation of elastic Young's modulus.

Spec. #	k	γ	λ^*	w	f_{md0}	f_{mdu}	ε_{md0}	ε_{mdu}
	-	-	-	mm	N/mm²	N/mm²	-	-
FEM-1S	1.046	1.50	1.737	636.4	1.70	0.40	0.001	0.008
FEM-2S	1.046	1.50	1.737	636.4	2.90	1.50	0.002	0.007
FEM-3S	1.046	1.50	1.737	636.4	0.80	0.15	0.001	0.008
FEM-1T	1.042	1.50	0.579	744.3	3.50	0.70	0.001	0.008
FEM-1T	1.044	1.50	1.158	673.8	3.20	1.40	0.002	0.006
FEM-1T	1.046	1.50	1.737	636.4	2.70	1.10	0.002	0.006
FEM-1T	1.048	1.50	2.316	611.7	2.20	1.20	0.001	0.006
FEM-1E	1.042	1.50	0.608	739.2	2.20	1.40	0.003	0.008
FEM-2E	1.044	1.50	1.169	672.8	2.30	1.40	0.002	0.005
FEM-3E	1.041	1.50	0.304	817.7	2.00	1.60	0.005	0.010
FEM-4E	1.050	1.50	2.734	598.2	2.50	1.45	0.001	0.005

Table 6: Identification parameters of equivalents strut models and stress-strain patameters.

5 PROPOSED CORRELATIONS TO DETERMINE STRESS-STRAIN PARAMETERS

The stress-strain parameters obtained from the calibration of the equivalent strut models on real experimental tests and FE simulations were used to define direct semi-empirical correlations linking geometric and mechanical data of an infilled frame to the parameters defining the equivalent strut stress-strain law. If one sets the following quantities:

$$\alpha = \frac{f_m^{\,2} \cdot w \cdot t \cdot \left(f_{vm} + \mu\sigma_n\right)}{\left(l/h\right) \cdot \lambda^{*0.4}} \tag{7}$$

$$\beta = \frac{f_{md0}^{\,0.8} \cdot w \cdot t}{E_{md}^{\,0.2} d} \tag{8}$$

$$\gamma = \left(\frac{f_{mdu}^{\,2}}{f_{md0}}\right)\left(\frac{E_c^{\,0.5}}{E_{md}^{\,1.5}}\right) \tag{9}$$

$$\delta = E_{md}^{\,0.15} \varepsilon_{md0} \tag{10}$$

where σ_n is the average compressive stress on masonry due to vertical loads while the meaning of the other symbols has been already explained, the following trends (Figure 10) can be observed with respect to the normalized stress-strain parameters f_{md0}/f_m, f_{mdu}/f_{md0}, $\varepsilon_{md0}/\varepsilon_{m0}$, $\varepsilon_{md}/\varepsilon_{md0}$ (ε_{m0} is set equal to 0.0015).

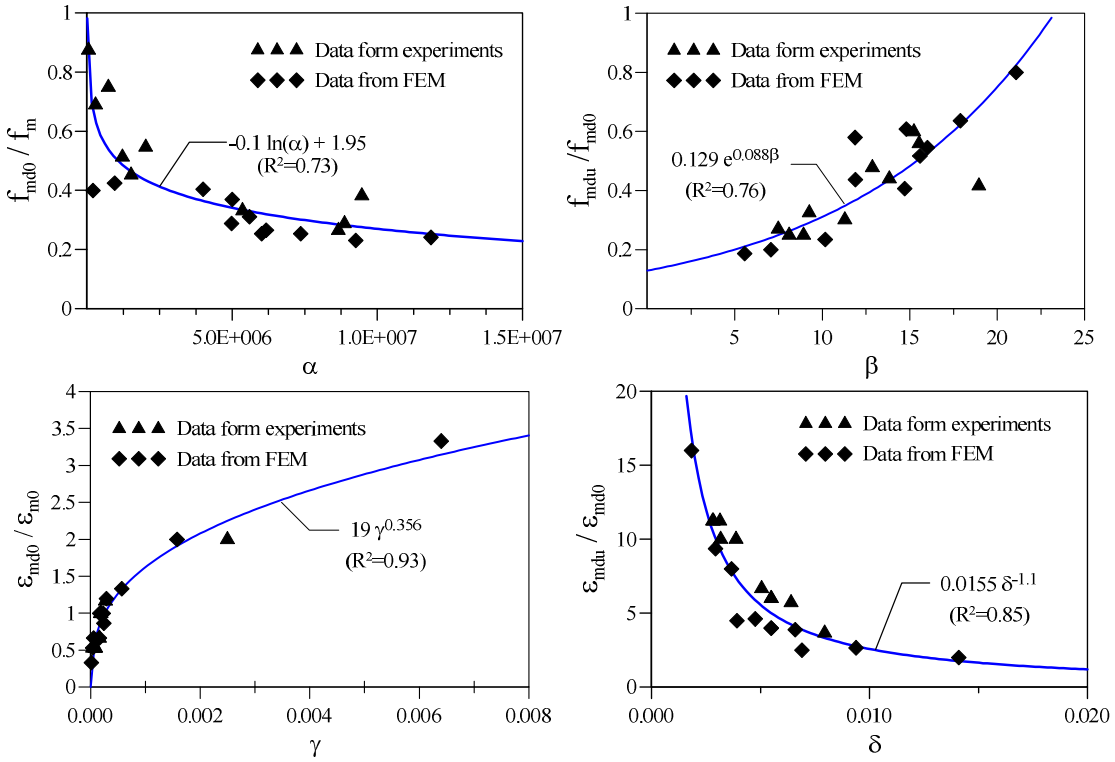

Figure 10: Relationship between parameters α, β, γ and δ and dimensionless stress-strain parameters and proposed analytical correlations.

Dimensionless stress-strain parameters resulted having a clear correlations with parameters α, β, γ and δ defined in Eqs. (7-10). These can be expressed by the following analytical relationships:

$$\frac{f_{md0}}{f_m} = -0.1 \cdot \ln(\alpha) + 1.95 \qquad (R^2 = 0.73) \tag{11}$$

$$\frac{f_{mdu}}{f_{md0}} = 0.129 \cdot e^{0.088\beta} \qquad (R^2 = 0.76) \tag{12}$$

$$\frac{\varepsilon_{md0}}{\varepsilon_{m0}} = 19 \cdot \gamma^{0.356} \qquad (R^2 = 0.93) \tag{13}$$

$$\frac{\varepsilon_{md0}}{\varepsilon_{mdu}} = 0.0155 \cdot \delta^{-1.1} \qquad (R^2 = 0.85) \tag{14}$$

The normalization of stress-strain parameters was adopted to highlight the relationship between the quantities. In this way the diagrams in Figure 10 give also the idea of the magnitude of variation between a stress-strain parameters and the entity used as normalizing factor.

In Eqs. (11-14) the coefficients of determination are also shown for each correlation. The latter range between 0.73 and 0.93, confirming an adequate reliability of the correlation laws proposed.

Stress-strain parameters of a generic infilled frame can be determined with Eqs. (7-10) and (11-14), which have to be used in the same order as they are listed. In fact paramter β depends on $f_{md0}=f(\alpha)$, paramter γ depends on $f_{mdu}=f(\beta)$ and parameter δ depends on $\varepsilon_{md0}=f(\gamma)$.

Eqs. (7-10), combined with Eqs. (11-14) can be used as an effective tool to predict the real complicated inelastic behaviour of an infilled frame subjected to lateral loads when using fiber-section equivalent strut macro models.

6 CONCLUSIONS

The identification of nonlinear behaviour of equivalent struts is still a major issue in the modeling process of infilled frames. This is due to the fact that the actual damage mechanisms activated in an infilled frame subjected to lateral loads can be really different and are not easy to be predicted a priori. Based on this, the paper proposes a method for the identification of the inelastic response of equivalents struts which starts from a semi-empirical approach oriented to the definition of concrete-type stress-strain relationship to be used for fiber-section modeling of equivalent struts. The parameters governing the equivalent strut stress-strain law, namely f_{md0}, ε_{md0}, f_{mdu}, ε_{mdu}, have been derived by iteratively calibrating a fiber-section equivalent strut model with real experimental tests and FE simulations. The stress strain-parameters have shown a distinct correlation with the quantities α, β, γ and δ, depending on simple geometric and mechanical features of the infilled frames. Analytical expressions describing such a correlation have been determined for each parameter, and have shown an adequate degree of reliability. The latter allow, through the simple evaluation of parameters α, β, γ and δ, to define the stress-strain parameters for a generic infilled frame. The identification strategy proposed on the paper can be used as a tool for the identification of the inelastic behaviour equivalents strut both for practical engineering and research purposes.

REFERENCES

[1] A.B. Mehrabi, P.B. Shing, M.P. Schuler, J.L. Noland, Experimental evaluation of masonry-infilled RC frames, *J Struct Eng (ASCE)*, **122**, No. 3, 228-37,1996.

[2] L. Cavaleri, F. Di Trapani, G. Macaluso, M. Papia, P. Colajanni, Definition of diagonal Poisson's ratio and elastic modulus for infill masonry walls, *Mat. and Struct.*, **47**(1-2), 239-262, 2014.

[3] D.J. Kakaletsis, C.G. Karayannis, Experimental investigation of infilled reinforced concrete frames with openings, *ACI Structural Journal*, **102**, No. 2, 132-141, 2009.

[4] L. Cavaleri, F. Di Trapani, G. Macaluso, M. Papia, Reliability of code proposed models for assessment of masonry elastic moduli, *Ingegneria Sismica*, Anno XXIX n.1. 2012.

[5] M. Dolšek, P. Fajfar, The effect of masonry infills on the seismic response of four storey reinforced concrete frame - a deterministic assessment, *Eng. Structures*, **30**, No. 7, 1991-2001, 2008.

[6] P.G. Asteris, C.C. Repapis, A.K Tsaris, F. Di Trapani, L. Cavaleri, Parameters affecting the fundamental period of infilled RC frame structures, *Earthquake and Structures*, **9**(5), 999-1028, 2015.

[7] P.G. Asteris, A.K. Tsaris, L. Cavaleri, C. Repapis, A. Papalou, F. Di Trapani, D.F. Karypidis,. Prediction of the Fundamental Period of Infilled RC Frame Structures Using Artificial Neural Networks, *Computational Intelligence and Neuroscience*, Article ID 474106, http://dx.doi.org/10.1155/2016/5104907, 2015.

[8] P.G. Asteris, Lateral Stiffness of Brick Masonry Infilled Plane Frames, *J. Struct. Eng. (ASCE)*, **129**, No. 8, 1071-1079, 2003.

[9] M. Papia, Analysis of infilled frames using a coupled finite element and boundary element solution scheme, *Int J Numerical Methods in Engineering*, **26**, No.3, 731-742, 1988.

[10] L. Cavaleri, F. Di Trapani, Prediction of the additional shear action on frame members due to infills, *Bulletin of Earthquake Engineering*, **13**(5), 1425-1454, 2015.

[11] I. Koutromanos, A. Stavridis, P.B. Shing, K. Willam, Numerical modelling of masonry-infilled RC frames subjected to seismic loads, *Computers and Structures* **89**, 1026-1037, 2011.

[12] A.B. Mehrabi, P.B. Shing, Finite element modelling of masonry-infilled RC frames, *J. Struct. Eng.*, **123**, No. 5, 604-13, 1997.

[13] A. Spada, G. Giambanco, P. Rizzo, Damage and plasticity at the interfaces in composite materials and structures, *Computer Methods in Applied Mechanics and Engineering*, **198**, No. 49-52, 3884 – 3901, 2009.

[14] G. Giambanco, G. Fileccia Scimemi, A. Spada, The interphase element, *Computational Mechanics*, **50**, No. 3, 353-366, 2012.

[15] B. Stafford Smith, C. Carter , A method for analysis for infilled frames, *Proc. of Institution of Civil Engineers*, Paper No.7218, 31-48, 1969.

[16] R.J. Mainstone, Supplementary note on the stiffness and strength of infilled frames, *Building Research Station*, Current Paper CP 13/74, UK.

[17] M. Papia, L. Cavaleri, M. Fossetti, Infilled frames: developments in the evaluation of the stiffening effect of infills, *Structural engineering and mechanics*, **16**, No. 6, 675-93, 2003.

[18] G. Campione, L. Cavaleri, G. Macaluso, G.Amato, F. Di Trapani, Evaluation of infilled frames: an updated in-plane-stiffness macro-model considering the effects of vertical loads, *Bulletin of Earthquake Engineering*, **13**(8), 2265-2281, 2015.

[19] P.G. Asteris, L. Cavaleri, F. Di Trapani, V. Sarhosis, A macro-modelling approach for the analysis of infilled frame structures considering the effects of openings and vertical loads, *Structure and Infrastructure Engineering,* **12**(5), 551-566, 2016.

[20] A. Saneinejad, B. Hobbs, Inelastic design of infilled frames, *J Struct Eng (ASCE)*, **121**, No. 4, 634-50, 1995.

[21] T.B. Panagiotakos, M.N. Fardis, Seismic response of infilled RC frames structures, *XXI WCEE*, Acapulco, Mexico, 1996.

[22] L. Cavaleri, F. Di Trapani, Cyclic response of masonry infilled RC frames: Experimental results and simplified modeling, *Soil Dynamics and Earthquake Engineering,* **65**, 224–242, 2014.

[23] A. Hashemi, K.M. Mosalam, Seismic Evaluation of Reinforced Concrete Buildings Including Effects of Masonry Infill Walls, *PEER Report*, University of California, Berkeley, 2007.

[24] S. Kadysiewski, K.M. Mosalam, Modeling of Unreinforced Masonry Infill Walls Considering In-Plane and Out-of-Plane Interaction, *PEER Report 2008/102*, University of California, Berkeley, January 2009.

[25] P.G. Asteris, L. Cavaleri, F. Di Trapani, A.K. Tsaris, Numerical modelling of out-of-plane response of infilled frames: State of the art and future challenges for the equivalent strut macromodels, *Engineering Structures*, **132**, 110-122, 2017.

[26] F. Di Trapani, G. Macaluso, L. Cavaleri, M. Papia, Masonry infills and RC frames interaction: literature overview and state of the art of macromodeling approach, *European Journal of Environmental and Civil Engineering*, **19**(9), 1059-1095, 2015.

[27] G. Campione, L. Cavaleri, F. Di Trapani, G. Macaluso, G. Scaduto, Biaxial deformation and ductility domains for engineered rectangular RC cross-sections: A parametric study highlighting the positive roles of axial load, geometry and materials, *Engineering Structures*, **107**(15), 116-134, 2016.

[28] P. Castaldo, B. Palazzo, Della Vecchia, Life-cycle cost and seismic reliability analysis of 3D systems equipped with FPS for different isolation degrees, *Engineering Structures*, **125**, 349-363, 2016.

[29] P. Castaldo, B. Palazzo, T. Ferrentino, Seismic reliability-based ductility demand evaluation for inelastic base-isolated structures with friction pendulum devices, *Earthquake Engineering and Structural Dynamics*, DOI: 10.1002/eqe.2854, 2016.

[30] P. Castaldo, B. Palazzo, A. Mariniello, Effects of the axial force eccentricity on the time-variant structural reliability of aging R.C. cross-sections subjected to chloride-induced corrosion, *Engineering Structures*, **130**, 261-274, 2017.

[31] P. Castaldo, G. Amendola, B. Palazzo, Seismic fragility and reliability of structures isolated by friction pendulum devices: seismic reliability-based design (SRBD), *Earthquake Engineering and Structural Dynamics*, **46**(3), 425-446, 2017.

[32] P. Castaldo, M. Ripani, Optimal design of friction pendulum system properties for isolated structures considering different soil conditions, *Soil Dynamics and Earthquake Engineering,* **90**, 74-87, 2016.

[33] D.C. Kent, R. Park, Flexural Members with Confined Concrete, *Journal of Structural Division ASCE*, **97**(7), 1969-90, 1971.
[34] F. McKenna, G.L. Fenves, M.H. Scott, *Open system for earthquake engineering simulation*, University of California, Berkeley, CA, 2000.
[35] M. Papia, L. Cavaleri, M. Fossetti, Infilled frames: developments in the evaluation of the stiffening effect of infills, *Structural engineering and mechanics*, **16**, No. 6, 675-93, 2003.